J Mol Model (2013) 19:3437–3446
DOI 10.1007/s00894-013-1845-5

ORIGINAL PAPER

Density functional studies on photophysical properties and chemical reactivities of the triarylboranes: effect of the constraint of planarity

Jun-Ling Jin · Hai-Bin Li · Tian Lu · Yu-Ai Duan · Yun Geng · Yong Wu · Zhong-Min Su

Received: 30 January 2013 / Accepted: 1 April 2013 / Published online: 25 May 2013

Abstract The geometric and electronic structures, absorption spectra, transporting properties, chemical reactivity indices and electrostatic potentials of the planar three-coordinate organoboron compounds **1**-**2** and twisted reference compound **Mes_3B**, have been investigated by employing density functional theory (DFT) and conceptual DFT methods to shed light on the planarity effects on the photophysical properties and the chemical reactivity. The results show that the planar compounds **1**-**2** exhibit significantly lower HOMO level than **Mes_3B**, owing to the stronger electronic induction effect of boron centers. This feature conspicuously induces a blue shifted absorption for **1**, although **1** seemingly possesses more extended conjugation framework than **Mes_3B**. Importantly, the reactivity strength of the boron atoms in **1**-**2** is much lower than that in **Mes_3B**, despite the fact that the tri-coordinate boron centers of **1**-**2** are completely naked. The interesting and abnormal phenomenon is caused by the strong p-π electronic interactions, that is, the empty p-orbital of boron center is partly filled by π-electron of the neighbor carbon atoms in **1**-**2**, which are confirmed by the analysis of Laplacian of the electron density and natural bond orbitals. Furthermore, the negative electrostatic potentials of the boron centers in **1**-**2** also interpret that they are not the most preferred sites for incoming nucleophiles. Moreover, it is also found that the planar compounds **1**-**2** can act as promising electron transporting materials since the internal reorganization energies for electron are really small.

Keywords Density functional calculations · Laplacian · Photophysics · Reactivity · Triarylborane

Introduction

Organic conjugated oligomers and polymers have stirred great attention for several decades due to their wide applications in the field of organic light-emitting diodes (OLEDs), as well as fluorescent probes, nonlinear optics, organic field-effect transistors (OFETs) [1, 2]. The fine-tuning of the photophysical properties and emission characteristics has established them as an important class of new materials with intriguing properties. In these issues, the incorporation of the main-group elements into the organic conjugated materials provides an opportunity to modify the properties of the luminescent systems, since the interactions between the atomic orbitals of main-group elements and the π-conjugation system endow the organic materials with promising properties [3–8]. In this regard, one of the most appealing aspects is the incorporation of the electron-deficient boron element into organic conjugated structures, which has emerged recently as promising materials for OLEDs and nonlinear optics [9–14]. In addition to the four-coordinate boron complexes, the three-coordinate organoboron compounds have demonstrated their application potentials in the real word [15–22]. The availability of the empty p_π orbital on the boron center and the extended π-system enable triarylboranes to show unusual optical and electronic properties. In resent years, many efforts have been devoted to designing and investigating the three-coordinate organoboron systems with novel properties

Electronic supplementary material The online version of this article (doi:10.1007/s00894-013-1845-5) contains supplementary material, which is available to authorized users.

J.-L. Jin · H.-B. Li · Y.-A. Duan · Y. Geng · Y. Wu · Z.-M. Su (✉)
Institute of Functional Material Chemistry, Faculty of Chemistry, Northeast Normal University, Changchun, China
e-mail: zmsu@nenu.edu.cn

T. Lu
Department of Chemistry and Chemical Engineering, School of Chemical and Biological Engineering, University of Science and Technology, Beijing, China

[23–25]. For instance, Yamaguchi and co-workers have recently shown that triarylboranes can be used as effective fluorescent sensors for Lewis donors such as fluoride [26, 27]. Shirota, Wang, Jäkle, and others have carried out extensive studies on the luminescent triarylboranes and have demonstrated their potential as effective emitters and electron-transporting materials [28–36].

In general, it is well known that the three-coordinate boranes are normally unstable toward hydrolysis by moisture. Therefore, the electron-deficient boron centers in the three-coordinate boranes need to be protected from external nucleophilic attack by using bulky substituents, such as phenyl, and 2,4,6-trimethylphenyl (mesityl) group. Kawashima and co-workers have synthesized several high-efficiency ladder-type azaborines using mesityl substituent to protect tri-coordinate boron atoms [37]. Moreover, Wagner and co-workers recently synthesized 9,10-dianthryl-9,10-dihydro-9,10-diboraanthracene with 9-anthyl moieties protecting boron atoms, and proved their good stability toward air and moisture [38]. Recently, Yamaguchi et al. reported a group of planarized triarylboranes, which exhibits completely planar geometries and has no bulky substituents for protecting the naked boron centers [39, 40]. To our surprise, these compounds are very stable toward moisture regardless of the naked boron centers, which is in sharp contrast to the traditional triarylboranes. Piers et al. proposed that the enforced planarity of the triarylboranes may be an effective mean of stabilizing kinetically naked boron centers [41]. However, the origin of the stability of the planarized triarylboranes is still unclear for researchers. Therefore, it is essential to disclose the planarity effects on the photophysical properties and chemical reactivities of triarylboranes for an in-depth understanding of the structure-property relationships, thus designing stable functional materials.

Currently, quantum chemistry investigations have proved to be an important avenue in revealing the origin of chemical and physical properties and to assist in designing new materials with ideal properties [42–46]. Therefore, in this work, a systematically theoretical study was performed to reveal the planarity effects on the photophysical properties of triarylboranes, and to provide insight into the origin of the stability of the planarized triarylboranes. Specifically, the reported compounds **1** and **2** (Fig. 1) were chosen as models, and conventional twisted compound **Mes_3B** (Fig. 1) was also considered for reference and comparison. Their geometric and electronic structures, optical spectra, orbital components, ionization energies (IEs), electron affinities (EAs), internal reorganization energies (λ_{int}), Fukui functions, condensed and local softness, and electrostatic potentials were explored using density functional theory (DFT) and conceptual DFT calculations to provide insight into the structure-property relationships and to understand the origin of the lowered reactivity of **1**-**2** toward nucleophiles.

Computational details

All calculations were performed using the Gaussian 09 package [48], unless otherwise stated. Comparative molecular structural calculations at the B3PW91/6-311+G(2df,2p) and B3PW91/6-31G(d,p) levels were carried out for **1**. The largest difference between the bond lengths of the two levels is less than 0.005 Å, indicating that the 6-31G(d,p) basis set used in this work is accurate enough. Therefore, the equilibrium structures of the studied compounds were optimized based on the experimental crystal structures [39, 49] using the B3PW91/6-31G(d,p) level for the sake of time efficiency. Harmonic vibrational frequencies were calculated following the optimizations to ensure that real minima were obtained. All the calculations were carried out without any symmetry constraints. The absorption spectra were systematically calculated by TD-DFT method at B3PW91/6-311+G(2d,p) level within the nonequilibrium polarizable continuum model (PCM) approach simulating the solvent effects (tetrahydrofuran, THF). In addition, the Fukui function [50, 51], local softness [52], dual descriptor [53], and Laplacian of the electron density were computed at B3PW91/6-31G(d,p) level through code Multiwfn 2.6 [54, 55] and their definition were summarized in Supporting information in detail. Generally, the adopted basis set affects the computed results of the Laplacian of the electron density. Luger et al. have demonstrated the influences of the basis sets on the calculated results of the Laplacian, *i.e.*, the more extended the basis is the more charge concentration is found in the bond. However, the computed values though different basis sets follow the same tendency within the studied compounds [56]. Therefore, the calculated results of Laplacian using B3PW91/6-31G(d,p) can provide reliable tendency for the studied compounds. The condensed descriptors, including condensed Fukui function, condensed softness, and condensed electrophilicity were calculated at B3PW91/6-31G(d,p) level using CHELPG scheme [57]. The electrostatic potentials (ESPs) for the studied compounds were computed at B3PW91/6-31G(d,p) level and were visualized using WFA Surface Analysis Suite [58]. The electronic configuration of boron centers were analyzed by natural bond orbitals (NBO) at B3PW91/6-31G(d,p) level.

Results and discussion

Geometric and electronic structures

The selected geometrical parameters optimized at the B3PW91/6-31G(d,p) level in gas phase together with the available X-ray crystal diffraction data are summarized in Table S1 (in Supporting information). The atomic labeling scheme is shown in Fig. 1. The relative errors between the

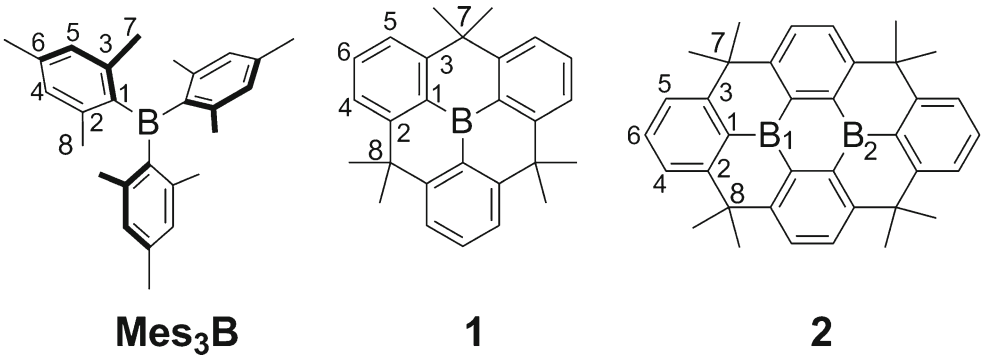

Fig. 1 The molecular structures of compounds **Mes$_3$B**, **1** and **2** and their numbering scheme

optimized bond lengths of **Mes$_3$B**, **1** and **2** and the corresponding experimental data are no more than 0.8 %, 0.7 %, and 0.7 %, respectively. Such discrepancies between the calculated and the experimental data are acceptable, indicating the B3PW91/6-31G(d,p) level can provide accurate prediction of the geometric structures. Notably, the bond length of B-C1 of **1** and **2** (1.523, 1.525 Å, respectively) is much shorter than that of **Mes$_3$B** (1.583 Å), indicating planarity strikingly impact the geometries of **1** and **2**. Furthermore, the significantly shorter bond lengths for B-C may be indicative of the strong interaction of the atomic orbitals for boron and carbon atoms in **1-2** (*vide infra*).

To evaluate preliminarily the effect of constraint planarity on the electron distribution in frontier molecular orbitals (FMOs), Fig. 2 shows the plots of highest occupied molecular orbital (HOMO) and the lowest unoccupied molecular orbital (LUMO), energy levels and the energy gaps for **Mes$_3$B**, **1** and **2** at their optimized S_0 geometries by B3PW91/6-31G(d,p) level in vacuum. As shown in Fig. 2, the distribution of HOMOs and LUMOs for **Mes$_3$B**, **1** and **2** present similar features. The LUMOs mainly locate on the center boron atom and phenyl fragments, while HOMOs are somewhat localized on the phenyl fragments for the three compounds. Nevertheless, from the twisted compound **Mes$_3$B** to the planar compounds **1-2**, their FMO energy levels are strikingly different. For **1**, the LUMO level is similar to that of **Mes$_3$B**, which is consistent with the experimental result [39]. However, the HOMO level is significantly lowered as compared to that of **Mes$_3$B**, although the conjugation of **1** seems to be more extended than that of **Mes$_3$B**. For **2**, the LUMO level is remarkably lowered, owing to the fact that **2** comprises two boron atoms which inherently hold the strong electron-withdrawing property. The HOMO level is slightly elevated compared

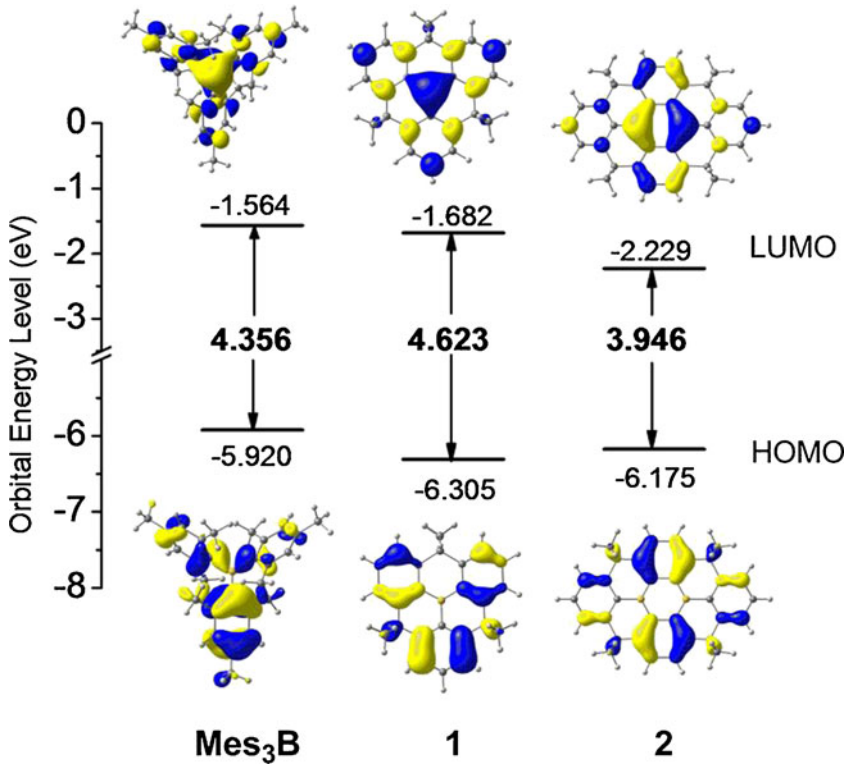

Fig. 2 The illustration of the orbital plots, the orbital energy levels, and the HOMO-LUMO energy gaps for compounds **Mes$_3$B**, **1** and **2** at their optimized S_0 geometries in vacuum at B3PW91/6-31G(d,p) level. The molecular orbital plots were obtained with an isosurface of 0.033 a.u. using ChemCraft [47]

with that of **1**, since the conjugation plane is extended. However, the HOMO of **2** is still much lower than that of **Mes$_3$B**. The significantly lowered HOMO for **1**-**2** must have close relationship with the planarity effects, which can be apparently characterized by the perturbation to the electron cloud distribution of HOMO for **1**. This interesting feature will be further revealed at the later section.

Absorption spectra and transporting properties

The absorption spectra calculated at PCM(THF)-B3PW91/6-311+G(2d,p) level were listed in Table 1. Moreover, to obtain more accurate results, a series of representative functionals including B3LYP [59, 60], B3PW91 [61–65], PBE0 [66–68], BMK [69], CAM-B3LYP [70], B971 [71], and M06 [72] were tested, taking **1** as an example. The calculated data and the experimental result collected in Table S2 (in Supporting information) show that B3PW91 provides the most accurate result, thus B3PW91 was adopted for the studied compounds. The calculated absorption wavelengths and the variation trends of the three compounds are in good agreement with experimental results, confirming that the adopted methods are reliable. The largest absorption lengths of the three compounds all originate from $S_0 \rightarrow S_1$ transition, mainly corresponding to the electron promotion from HOMO to LUMO. The largest absorption wavelength of **1** (313.3 nm) is blue shifted compared to that of **Mes$_3$B** (352.9 nm), demonstrating the perturbation of conjugation caused by planarity effects. **2** shows a strikingly red shifted absorption band than those of **1** and **Mes$_3$B**, which can be explained by its narrow band gap. Consequently, planarity effects exert pronounced influence on the optical properties of **1**-**2**.

Ionization energies (IEs), electron affinities (EAs), and internal reorganization energies for hole (λ_{int}^{+}) and electron (λ_{int}^{-}) of **Mes$_3$B**, **1** and **2** have been calculated at B3PW91/6-31G(d,p) level to evaluate their transporting properties, and the results were listed in Table 2. From the computed results, the values of IEs for **Mes$_3$B**, **1** and **2** are relatively large, manifesting that it is rather difficult for hole injection due to the high barrier of injection [73]. Therefore, **1** and **2** can be used as potential hole-blocking materials in the OLEDs. In addition, the values of EAs for **1** and **2** are small, indicating the good ability of catch electron. Especially, it is important to note that the difference between the vertical and adiabatic IEs (EAs) for **1** and **2** is much smaller than that of **Mes$_3$B**. This fact implies that after gaining (or losing) electron, **1** and **2** undergo a smaller structural relaxation than **Mes$_3$B**, which is very important for the charge mobility. On the other hand, the planar configurations normally facilitate charge transport since they tend to prefer the tightly-stacked packing motifs and strong intermolecular electronic coupling [44, 74, 75]. Therefore, planar compounds **1** and **2** will facilitate the electron transport rather than **Mes$_3$B**. More importantly, from the computed results of internal reorganization energy, **1** and **2** both possess conspicuously smaller reorganization energies for electron (0.083, 0.116 eV for **1** and **2**, respectively) than that of **Mes$_3$B** (0.212 eV). The values of λ_{int}^{-} for **1**-**2** are even lower than those of perylene bisimide (PDI) derivatives (*ca.* 0.3 eV, obtained at B3LYP/6-31G(d,p) level) [76], which are typical electron transporting materials. This conceivably supports that **1** and **2** could act as better electron-transport materials. However, three-coordinate boranes are normally unstable due to the reactivity of the electron-deficient boron atoms. Therefore, the chemical reactivities of the **1**-**2** and the reference compound **Mes$_3$B** were characterized in detail in the next section.

Table 2 The calculated vertical and adiabatic ionization energies (IEs) and electron affinities (EAs), internal reorganization energies for hole (λ_{int}^{+}) and electron (λ_{int}^{-}) of compounds **Mes$_3$B**, **1** and **2**. All values in eV

Compound	IE_v	IE_a	EA_v	EA_a	λ_{int}^{+}	λ_{int}^{-}
Mes$_3$B	7.288	7.158	0.556	0.447	0.260	0.212
1	7.644	7.583	0.376	0.417	0.124	0.083
2	7.347	7.296	1.054	1.111	0.106	0.116

Reaction activity

In recent years, within the context of DFT, many useful and important reactivity indices, such as Fukui function, electronegativity, hardness, and softness, have provided reliable interpretations and predictions of chemical reactivity sites and the mechanism of the chemical reactions [77–86]. To

Table 1 Calculated absorption (λ_{abs}, nm) wavelengths, excitation energies (E_x, eV), oscillator strengths *f*, and dominant excitation character of **Mes$_3$B**, **1** and **2** together with experimental results ($\lambda_{exp.}$, nm). Calculations were performed at PCM(THF)-TD-B3PW91/6-311+G(2d,p)//B3PW91/6-31G(d,p) level

Compound	Transition	λ_{abs}	E_x	*f*	Composition[a]	$\lambda_{exp.}$[b]
Mes$_3$B	$S_0 \rightarrow S_1$	352.9	3.513	0.136	H→L (98 %)	332
1	$S_0 \rightarrow S_1$	313.3	3.957	0.108	H→L (95 %)	320
2	$S_0 \rightarrow S_1$	370.4	3.347	0.212	H→L (97 %)	377

[a] H denotes HOMO and L denotes LUMO [b] Measured in THF, ref. [39]

find the most preferred site for nucleophilic attack, the dual descriptor Δf, Fukui function and local softness toward nucleophiles (f^+ and s^+) were calculated at B3PW91/6-31G(d,p) level using code Multiwfn 2.6 [54, 55] and the results were illustrated in Fig. 3. All the plots of Δf, f^+, and s^+ show that the maximum site is on the boron atoms for the three compounds, demonstrating the reactivity of boron atoms for nucleophilic attack. However, the contribution from the boron center to the Fukui function and local softness clearly decreases from **Mes_3B** to **1**-**2**, which is indicative of the lowered reactivity toward nucleophiles for the latter two compounds. This is in good agreement with the experimental results. Furthermore, it is observed from the plots of Δf that **Mes_3B** shows evidently negative Δf (favored for electrophilic attack) regions at C1 species, while those in **1**-**2** are remarkably small, suggesting **Mes_3B** also shows relatively stronger reactivity toward electrophiles.

To more clearly compare the chemical reactivity strength of the boron centers, a series of condensed descriptors for reactivity, including condensed Fukui function, condensed softness, and condensed electrophilicity has been computed using CHELPG scheme [57]. Generally, the condensed reactivity descriptors are sensitive to the adopted method and population partitioning scheme. From the previous works, the choice of DFT methods based on exchange correlation functional is crucial for the calculation of the condensed descriptors [78]. In 2002, Subramanian et al. had investigated the effects of the basis set and population scheme on the results of the condensed Fukui functions [87]. Their results showed that CHELPG is a reliable scheme and could provide precise reactive site with less dependency on the basis sets. Therefore, all the condensed descriptors were calculated at B3PW91/6-31G(d,p) level for the sake of computational cost. The condensed softness, which combines local (atomic) and global information for a molecule, is strikingly important for the interpretation of reactions for the same sites in different molecules [88]. It has been found that for frontier orbital controlled soft-soft interactions, the increasing condensed softness of the contact atom will result in an increase of the chemical reactivity [81]. From Table 3, evidently, the reactivity of the boron atom for **Mes_3B** is much higher than those of **1** and **2**, since the values of the condensed softness are much larger for boron center in **Mes_3B**. The reactivity of the boron atoms for nucleophilic attack decreases in the order of **Mes_3B** > **1** > **2**. This feature can also be reflected by the atomic charge values (q) for the boron atom. The atomic charge of **Mes_3B** is more positive than **1**-**2**, demonstrating the stronger electrostatic attraction to the incoming nucleophiles. Moreover, **Mes_3B** presents a condensed electrophilicity value of $\omega^+(B) = 0.593$ at boron center. However, the constraint planarity decreases the condensed electrophilicity power of

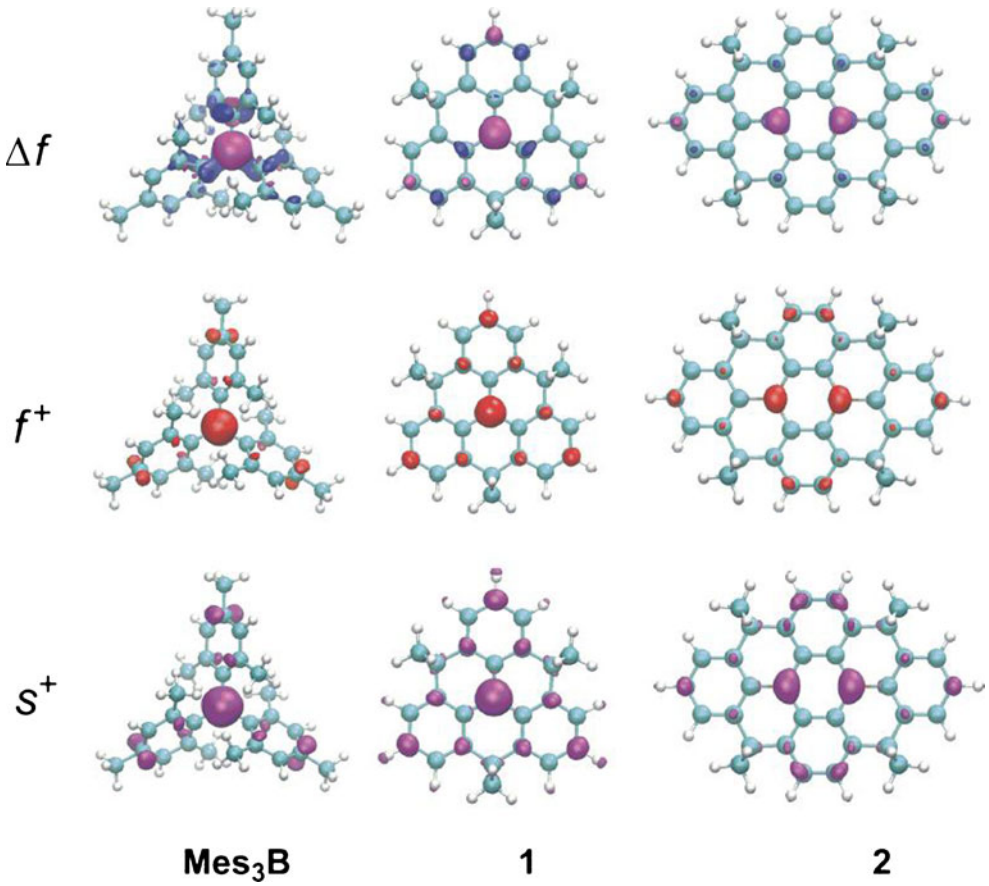

Fig. 3 The maps of dual descriptor (Δf), Fukui function (f), and local softness (s) toward nucleophilic attack for **Mes_3B**, **1** and **2**. The isosurfaces surface of Δf, f^+, and s^+ is 0.0032, 0.0032, and 0.0003 a.u., respectively. For the plots of Δf, purple is positive zone and blue is negative zone

Table 3 The computed results of chemical hardness (η, eV), chemical potential (μ, eV), electrophilicity index (ω, eV) and global softness (S, eV^{-1}) for **Mes_3B**, **1** and **2**. Condensed Fukui functions (f^+, a.u.), softness (s^+, $a.u.eV^{-1}$), and electrophilicity (ω^+, a.u. eV) of the contact boron atom using CHELPG method are also listed. All the values were computed at B3PW91/6-31G(d,p) level

Compound	η	μ	ω	S	q(B)	f^+(B)	s^+(B)	ω^+(B)
Mes_3B	6.841	−3.868	1.093	0.146	0.710	0.542	0.079	0.593
1	7.268	−4.010	1.106	0.138	0.344	0.457	0.063	0.506
2[a]	6.293	−4.201	1.402	0.159	0.307	0.243	0.039	0.341

[a] For **2**, the related condensed values for B2 are same to B1

boron center from 0.593 in **Mes_3B** to 0.506 in **1**. Note that the condensed local electrophilicity for boron atom is mainly derived by change in the condensed Fukui function. Consequently, the boron centers of **1**-**2** show relatively lower reactivity toward nucleophiles compared to that of **Mes_3B**, which agree well with the experimental findings.

It is well-known that the three-coordinate boranes normally need bulky substituents to protect the electron-deficient boron atom from nucleophilic attack. Surprisingly, the boron centers in **1**-**2** are more stable toward nucleophilic attack than that in **Mes_3B** according to the calculated results, although the empty p_π orbital of the boron center is completely naked. To reveal the origin of this interesting and abnormal phenomenon, we will next look at the Laplacian of the electron density and electrostatic potential.

Laplacian of the electron density and electrostatic potential

To unveil the origin of the lowered reactivity of the boron centers in **1**-**2**, the components of their LUMOs were first analyzed and the result was plotted in Fig. 4. As discussed above, the boron center makes negligible contribution to the HOMO, while its contribution to LUMO is strikingly different for **Mes_3B**, **1** and **2** (see Fig. 2). Figure 4 shows that the contribution of the boron is greatly reduced from **Mes_3B** to **1**. Turning from **1** to **2**, the contribution of the boron atoms to the LUMO is slightly higher, owing to the fact that **2** has two boron atoms. Note that the contribution of boron for **2** is still smaller than that for **Mes_3B**, again proving that the planar configurations facilitate the extension the π-conjugation electron and stabilize the empty p orbital of the boron center.

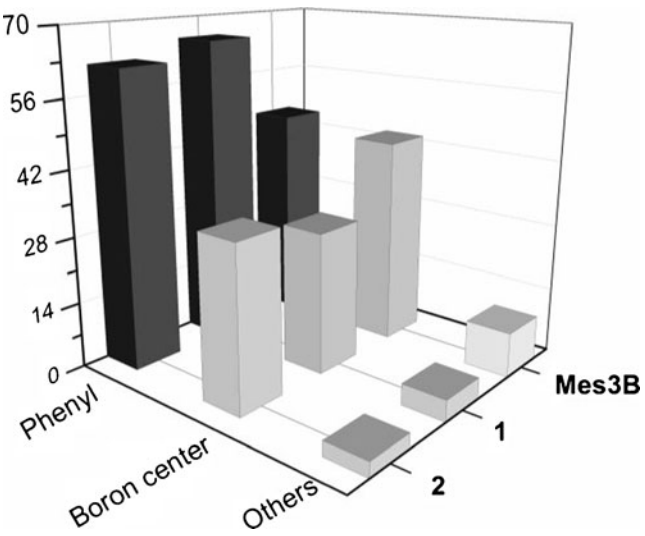

Fig. 4 The lowest unoccupied molecular orbital (LUMO) components (including three parts: boron, phenyl, and others, in percent) for compounds **Mes_3B**, **1** and **2** at optimized S_0 geometries in vacuum at B3PW91/6-31G(d,p) level

Laplacian of the electron density $\nabla^2\rho(r)$ is a useful tool for characterizing bonding interactions [89–94]. The investigation of the Laplacian of electron density could also provide insight into the electronic properties of atoms and molecules, and allow for useful predictions of chemical reactivity [95–99]. In general, regions where the Laplacian is negative reflect the charge is locally concentrated, which are characteristic of covalent bonding interactions. Conversely, regions where the Laplacian is positive indicate the charge is depleted, which are typical of closed-shell interactions. For the sites with negative Laplacian, they tend to deliver electronic charge and reactive toward electrophilic reactants, while those with positive Laplacian, they are apt to accommodate extra electronic charge and reactive toward nucleophilic reactants [93].

The Laplacian of the electron density shown in Fig. 5 has been computed at B3PW91/6-31G(d,p) level using code Multiwfn 2.6 [54, 55]. In addition, Wiberg bond index (WBI), which is a useful description of delocalization [100–102], was also computed to gain further insights into the bonding situation and the results were collected in Table S3 (Supporting information). It is readily seen from the plots of Fig. 5 and Fig. S1 that the carbon atoms of the phenyl ring are sp^2 hybridized and the electron-rich regions locate around carbon atoms for **Mes_3B**, **1**, and **2**. The electron-depleted region (electron-poor zone) is found in center boron atom, confirming the electron-deficient characteristic of boron center. It is evident that the boron center is stabilized by the charge-concentrated neighbor carbon atoms. Interestingly, the extension of the charge concentration region in B-C1 bond for **1** and **2** is much greater than that for **Mes_3B**,

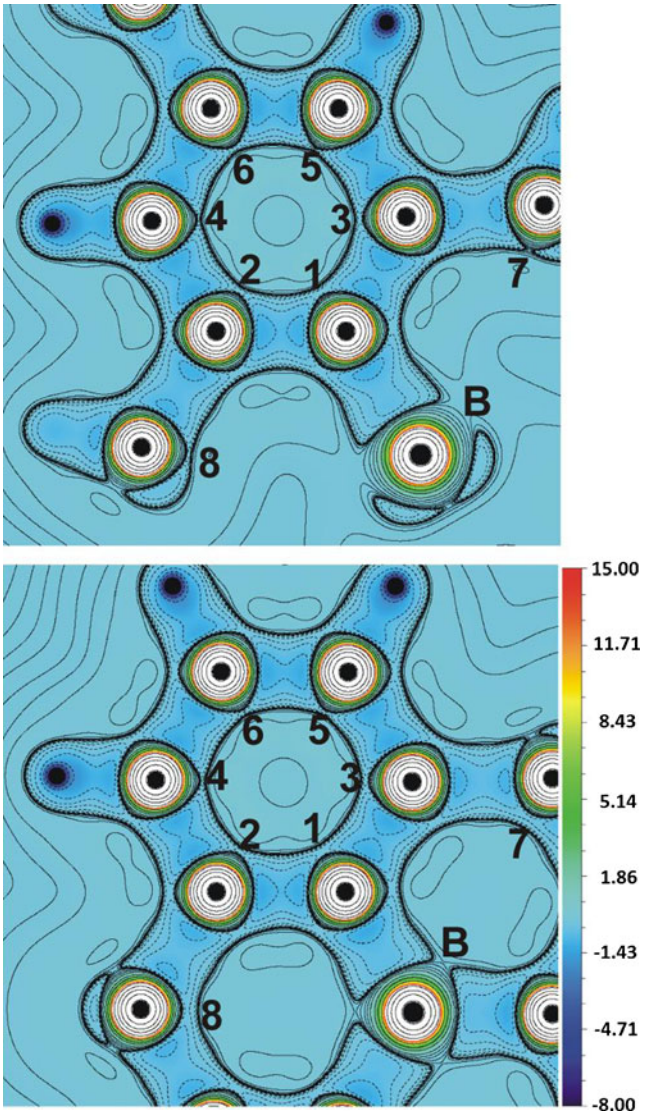

Fig. 5 Contour maps of the Laplacian of the electron density ($\nabla^2\rho$) for **Mes_3B** (*top*) and **1** (*bottom*), in the plane defined by atoms B, C1 and C2 (The Laplacian of **2** resembles that of **1**, hence the related plots was presented in supporting information). The dash lines denote negative Laplacian, while the solid lines denote positive Laplacian

manifesting that the interactions between boron center and neighbor carbon atoms are much stronger for **1** and **2**. The relatively stronger interatomic orbital interactions in **1**-**2** also can be indicated by the larger values of WBI for B-C1 (0.949, 0.951, 0.888 for **1**, **2**, **Mes_3B**, respectively). More importantly, the delocalization of π electron in C1 atoms into the vacant p orbital in boron center can be further proved by the calculation results of natural bond orbitals (NBO) analysis. The electronic configuration of boron atom is $2s(0.62)2p(1.47)$ for **Mes_3B**, while those for **1**-**2** are $2s(0.57)2p(1.68)$, $2s(0.58)2p(1.65)$ (B1 in **2**), 2s(0.58)2*p*(1.65) (B2 in **2**), respectively. The net electrons for boron atoms in **1**-**2** are clearly larger than that in **Mes_3B**, suggesting that the empty p_π orbital has been partly filled for **1**-**2**. Therefore, the stabilization effects provided by charge-concentrated C1 species are much greater in **1**-**2** than those in **Mes_3B**. This feature is strikingly important for the lowered reactivity toward nucleophiles for **1**-**2**, whose boron centers is naked without any protection of bulky substituents and shows higher stability toward nucleophilic attack.

For carbon atoms C7 and C8 in **1** and **2**, the extension of charge concentrated zone for C7-C3 and C8-C2 is smaller than the bonds of the phenyl ring (such as C2-C4, C4-C6, etc.). The related bonds associated to C7 and C8 do not participate in the conjugation system, since they have single bond character as manifested by WBI values which are close to 1.0. Importantly, for the three compounds the extension of charge concentrated region in the bonds of C1-C2 and C1-C3 is different from those of C2-C4, C3-C5, C4-C6, and C5-C6, where the former are relatively smaller than the later. Moreover, the computed nucleus independent chemical shift (NICS) values at the geometric center phenyl rings calculated at B3LYP/6-31+G(d,p) level for **1** and **2** (−6.78 and −6.57) are much higher than that of benzene (−8.04) [103, 104]. These characteristics manifest boron atoms which strikingly disturb the conjugation system. The charge-depleted boron atoms in **1** and **2** clearly have no contribution to the conjugation system. In converse, the empty p_π orbital of boron center needs to be stabilized by the conjugation system. Coincidentally, the planar configuration of **1** and **2** is beneficial for the boron center extract electron from

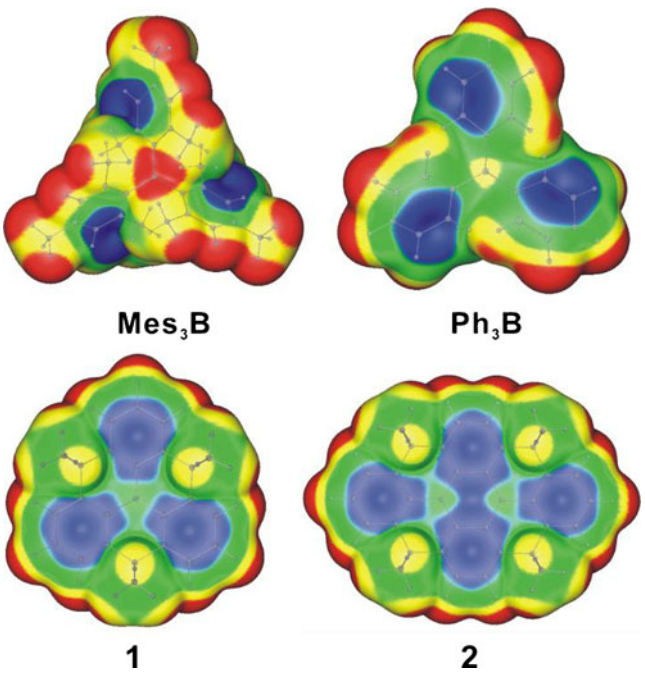

Fig. 6 The electrostatic potential (in a.u.) of compounds **Mes_3B**, **Ph_3B**, **1** and **2** calculated at B3PW91/6-31G(d,p) level. The electrostatic potential values are mapped on the surface of electron density (0.001 a.u.) and created with WFA Surface Analysis Suite [58]. Color range: blue <−0.017, green −0.017 ─ 0, yellow 0 ─ 0.010, red >0.010

neighbor carbon atoms. This also can be characterized by the relatively smaller value of the EA_v for **1** (0.376 eV for **1** and 0.556 eV for **Mes$_3$B**), which suggests the electron-deficient boron atom has been stabilized. Therefore, the HOMO level of **1** is lowered compared to that of **Mes$_3$B**, although they possess similar conjugation framework (*vide supra*). In addition, to clarify the contribution of the conjugation and inductive effects to the lowered HOMO of **1** and **2**, the simplest arylborane compound, $C_6H_5BH_2$, was calculated. The planar and twisted (the BH_2 subunit is perpendicular to benzene plane) $C_6H_5BH_2$ model and the calculation details were presented in the Supporting information (Fig. S2). The HOMO level is −7.14 and −6.64 eV for the planar and twisted model, respectively, which exhibit similar tendency as **1** and **Mes$_3$B**. For the planar model, the electronic configuration of boron atom is $2s(0.85)2p_x(0.71)$ $2p_y(0.90)$ $2p_z(0.14)$, while the twisted model is $2s$ $(0.87)2p_x(0.72)$ $2p_y(0.02)$ $2p_z(0.88)$. This feature indicates that the conjugation effects of the boron center are more important for the lowered HOMO.

Additionally, within the framework of hard and soft acids and bases of Pearson [105, 106], the electrostatic potential (ESP), which is frequently used to predict the reactive sites for hard-hard interactions and the packing motifs of a crystal [107–110], has been computed (at B3PW91/6-31G(d,p) level in vacuum) for **Mes$_3$B**, **1** and **2**. The most positive (negative) regions of ESP are generally preferred for nucleophilic (electrophilic) attack. From the plots of Fig. 6, the hydrogen atoms present the most positive ESP regions, while the conjugated systems (phenyl rings) show the most negative regions for the three compounds. Interestingly, the boron centers of the planar compounds **1**-**2** take negative electrostatic potential values, which is less negative than those of conjugated systems. This proves that the boron centers are not the most preferred sites for nucleophilic attack, in line with the above discussions of the reactivity descriptors. It is well-known that the boron center of **Mes$_3$B** is well protected by methyls in mesityl groups. The positive ESP regions near the boron center in **Mes$_3$B** are probably attributed to the hydrogen atoms in methyl groups. Therefore, the ESP of the triphenylboron (**Ph$_3$B** in Fig. 6) was also computed to distinctly compare the ESP behaviors of the boron centers. From Fig. 6, the boron center of the **Ph$_3$B** clearly presents a positive ESP value, demonstrating the high reactivity toward nucleophiles. This further confirms that the planarity effects strikingly reduce the strength of the chemical reactivity for boron atoms toward nucleophiles.

Conclusions

The aim of the present investigation was to assess the planarity effects on the photophysical properties and the chemical reactivities of three-coordinate organoboron compounds **1**-**2** as compared to the twisted reference compound **Mes$_3$B**. To this end, within the framework of DFT and conceptual DFT the geometric and electronic structures, absorption spectra, ionization energies and electron affinities, chemical reactivity indices and electrostatic potentials have been calculated. The results can well reproduce the experimental measurements. With the planarity configurations, **1** exhibits significantly lower HOMO level than **Mes$_3$B**, owing to the stronger electronic induction effect of boron center. The characteristic directly induces a blue shifted absorption for **1** compared with **Mes$_3$B**, although **1** seemingly possesses more extended conjugation framework than **Mes$_3$B**. **1**-**2** can act as promising electron transporting materials since their reorganization energies for electron are really small. Interestingly, the completely naked boron atoms of **1**-**2** are more stable toward nucleophiles than the well protected one in **Mes$_3$B** according to the calculated chemical reactivity indices. This interesting and abnormal phenomenon can be explained by the stronger electronic interactions between boron center and neighbor carbon atoms in **1**-**2**, which are confirmed by the analysis of Laplacian of the electron density and NBO. Furthermore, the negative electrostatic potentials of the boron centers in **1**-**2** also rationalized the lowered chemical reactivity.

Acknowledgments We gratefully acknowledge financial support from National Natural Science Foundation of China (NSFC 21273030 and 21203019), 973 Program (2009CB623605), Specialized Research Fund for the Doctoral Program of Higher Education (SRFDP) and Research Grants Council Earmarked Research Grants (RGC ERG) Joint Research Program (20120043140001) and the Science and Technology Development Planning of Jilin Province (201201071).

References

1. Mishra A, Ma CQ, Bäuerle P (2009) Chem Soc Rev 109:1141–1276
2. Lo SC, Burn PL (2007) Chem Soc Rev 107:1097–1116
3. Xu C, Wakamiya A, Yamaguchi S (2005) J Am Chem Soc 127:1638–1639
4. Mouri K, Wakamiya A, Yamada H, Kajiwara T, Yamaguchi S (2006) Org Lett 9:93–96
5. Yamaguchi S, Endo T, Uchida M, Izumizawa T, Furukawa K, Tamao K (2000) Chem Eur J 6:1683–1692
6. Fukazawa A, Yamada H, Yamaguchi S (2008) Angew Chem Int Ed 47:5582–5585
7. Furukawa S, Kobayashi J, Kawashima T (2010) Dalton Trans 39:9329–9336
8. Jacquemin D, Quinet O, Champagne B, André JM (2004) J Chem Phys 120:9401–9409
9. Campbell PG, Marwitz AJV, Liu SY (2012) Angew Chem Int Ed 51:6074–6092
10. Entwistle CD, Marder TB (2002) Angew Chem Int Ed 41:2927–2931
11. Le Guennic B, Maury O, Jacquemin D (2012) Phys Chem Chem Phys 14:157–164
12. Jin JL, Li HB, Geng Y, Wu Y, Duan YA, Su ZM (2012) ChemPhysChem 13:3714–3722

13. Jacquemin D, Lambert C, Perpète EA (2003) Macromolecules 37:1009–1015
14. Jin JL, Wu SX, Geng Y, Yang SY, Yang GC, Wu J, Muhammad S, Liao Y, Su ZM, Hao LZ (2012) Int J Quantum Chem 112:440–452
15. Hudson ZM, Wang S (2009) Acc Chem Res 42:1584–1596
16. Nishida J-I, Fujita T, Fujisaki Y, Tokito S, Yamashita Y (2011) J Mater Chem 21:16442–16447
17. Zhou Z, Yang H, Shi M, Xiao S, Li F, Yi T, Huang C (2007) ChemPhysChem 8:1289–1292
18. Robinson S, McMaster J, Lewis W, Blake AJ, Liddle ST (2012) Chem Commun 48:5769–5771
19. Zhao CH, Wakamiya A, Inukai Y, Yamaguchi S (2006) J Am Chem Soc 128:15934–15935
20. Sundararaman A, Venkatasubbaiah K, Victor M, Zakharov LN, Rheingold AL, Jäkle F (2006) J Am Chem Soc 128:16554–16565
21. Agou T, Kobayashi J, Kawashima T (2007) Chem Eur J 13:8051–8060
22. Iida A, Sekioka A, Yamaguchi S (2012) Chem Sci 3:1461–1466
23. Weber L, Eickhoff D, Marder TB, Fox MA, Low PJ, Dwyer AD, Tozer DJ, Schwedler S, Brockhinke A, Stammler HG, Neumann B (2012) Chem Eur J 18:1369–1382
24. Marwitz AJV, Lamm AN, Zakharov LN, Vasiliu M, Dixon DA, Liu SY (2012) Chem Sci 3:825–829
25. Thanthiriwatte KS, Gwaltney SR (2006) J Phys Chem A 110:2434–2439
26. Yamaguchi S, Shirasaka T, Akiyama S, Tamao K (2002) J Am Chem Soc 124:8816–8817
27. Zhao CH, Sakuda E, Wakamiya A, Yamaguchi S (2009) Chem Eur J 15:10603–10612
28. Sun Y, Ross N, Zhao S-B, Huszarik K, Jia WL, Wang R-Y, Macartney D, Wang S (2007) J Am Chem Soc 129:7510–7511
29. Entwistle CD, Marder TB (2004) Chem Mater 16:4574–4585
30. Doi H, Kinoshita M, Okumoto K, Shirota Y (2003) Chem Mater 15:1080–1089
31. Kinoshita M, Kita H, Shirota Y (2002) Adv Funct Mater 12:780–786
32. Shirota Y, Kinoshita M, Noda T, Okumoto K, Ohara T (2000) J Am Chem Soc 122:11021–11022
33. Weber L, Werner V, Fox MA, Marder TB, Schwedler S, Brockhinke A, Stammler H-G, Neumann B (2009) Dalton Trans 38(15):2823–2831
34. Chen P, Jäkle F (2011) J Am Chem Soc 133:20142–20145
35. Fu GL, Zhang HY, Yan YQ, Zhao CH (2012) J Org Chem 77:1983–1990
36. Sun C, Hudson ZM, Helander MG, Lu ZH, Wang S (2011) Organometallics 30:5552–5555
37. Agou T, Kobayashi J, Kawashima T (2007) Chem Commun 43(30):3204–3206
38. Januszewski E, Lorbach A, Grewal R, Bolte M, Bats JW, Lerner H-W, Wagner M (2011) Chem Eur J 17:12696–12705
39. Zhou Z, Wakamiya A, Kushida T, Yamaguchi S (2012) J Am Chem Soc 134:4529–4532
40. Saito S, Matsuo K, Yamaguchi S (2012) J Am Chem Soc 134:9130–9133
41. Araneda JF, Neue B, Piers WE (2012) Angew Chem Int Ed 51:9977–9979
42. Adamo C, Jacquemin D (2013) Chem Soc Rev 42:845–856.
43. Brédas J-L, Norton JE, Cornil J, Coropceanu V (2009) Acc Chem Res 42:1691–1699
44. Duan YA, Geng Y, Li HB, Tang XD, Jin JL, Su ZM (2012) Org Electron 13:1213–1222
45. Thomas A, Krishna Chaitanya G, Bhanuprakash K, Krishna Prasad KMM (2011) ChemPhysChem 12:3458–3466
46. Zhang J, Kan Y-H, Li H-B, Geng Y, Wu Y, Su Z-M (2012) Dye Pigment 95:313–321
47. ChemCraft, Version 1.6 (build 356). (2012) http://www.chemcraftprog.com/
48. Frisch MJ, Trucks GW, Schlegel HB, Scuseria GE, Robb MA, Cheeseman JR, Scalmani G, Barone V, Mennucci B, Petersson GA, Nakatsuji H, Caricato M, Li X, Hratchian HP, Izmaylov AF, Bloino J, Zheng G, Sonnenberg JL, Hada M, Ehara M, Toyota K, Fukuda R, Hasegawa J, Ishida M, Nakajima T, Honda Y, Kitao O, Nakai H, Vreven T, Montgomery JA Jr, Peralta JE, Ogliaro F, Bearpark M, Heyd JJ, Brothers E, Kudin KN, Staroverov VN, Kobayashi R, Normand J, Raghavachari K, Rendell A, Burant JC, Iyengar SS, Tomasi J, Cossi M, Rega N, Millam JM, Klene M, Knox JE, Cross JB, Bakken V, Adamo C, Jaramillo J, Gomperts R, Stratmann RE, Yazyev O, Austin AJ, Cammi R, Pomelli C, Ochterski JW, Martin RL, Morokuma K, Zakrzewski VG, Voth GA, Salvador P, Dannenberg JJ, Dapprich S, Daniels AD, Farkas O, Foresman JB, Ortiz JV, Cioslowski J, Fox DJ (2009) Gaussian 09 W: Revision A.02. Gaussian, Inc, Wallingford
49. Olmstead MM, Power PP (1986) J Am Chem Soc 108:4235–4236
50. Parr RG, Yang W (1984) J Am Chem Soc 106:4049–4050
51. Ayers PW, Parr RG (2000) J Am Chem Soc 122:2010–2018
52. Chattaraj PK, Sarkar U, Roy DR (2006) Chem Soc Rev 106:2065–2091
53. Morell C, Grand A, Toro-Labbé A (2004) J Phys Chem A 109:205–212
54. Lu T (2012) Multiwfn version 2.6. A multifunctional wavefunction analyzer http://multiwfn.codeplex.com
55. Lu T, Chen F (2012) J Comput Chem 33:580–592
56. Flaig R, Koritsanszky T, Zobel D, Luger P (1998) J Am Chem Soc 120:2227–2238
57. Breneman CM, Wiberg KB (1990) J Comput Chem 11:361–373
58. Bulat F, Toro-Labbé A, Brinck T, Murray J, Politzer P (2010) J Mol Model 16:1679–1691
59. Becke AD (1993) J Chem Phys 98:1372–1377
60. Lee C, Yang W, Parr RG (1988) Phys Rev B 37:785–789
61. Perdew JP (1991) Electronic structure of solids '91. Akademie, Berlin
62. Perdew JP, Chevary JA, Vosko SH, Jackson KA, Pederson MR, Singh DJ, Fiolhais C (1993) Phys Rev B 48:4978
63. Perdew JP, Burke K, Wang Y (1996) Phys Rev B 54:16533–16539
64. Perdew JP, Chevary JA, Vosko SH, Jackson KA, Pederson MR, Singh DJ, Fiolhais C (1992) Phys Rev B 46:6671–6687
65. Dobson JF, Vignale G, Das P (1998) Electronic density functional theory: recent progress and new directions. Plenum Press, New York
66. Perdew JP, Burke K, Ernzerhof M (1996) Phys Rev Lett 77:3865–3868
67. Perdew JP, Burke K, Ernzerhof M (1997) Phys Rev Lett 78:1396(E)
68. Adamo C, Barone V (1999) J Chem Phys 110:6158–6170
69. Boese AD, Martin JML (2004) J Chem Phys 121:3405–3416
70. Yanai T, Tew DP, Handy NC (2004) Chem Phys Lett 393:51–57
71. Halgren TA, Lipscomb WN (1977) Chem Phys Lett 49:225–232
72. Zhao Y, Truhlar DG (2008) Theor Chem Accounts 120:215–241
73. Gao H, Qin C, Zhang H, Wu S, Su ZM, Wang Y (2008) J Phys Chem A 112:9097–9103
74. Koh SE, Risko C, da Silva Filho DA, Kwon O, Facchetti A, Brédas JL, Marks TJ, Ratner MA (2008) Adv Funct Mater 18:332–340
75. Geng Y, Wu SX, Li HB, Tang XD, Wu Y, Su ZM, Liao Y (2011) J Mater Chem 21:15558–15566
76. Geng Y, Wang J, Wu S, Li H, Yu F, Yang G, Gao H, Su Z (2011) J Mater Chem 21:134–143
77. De Proft F, Geerlings P (2001) Chem Soc Rev 101:1451–1464
78. Geerlings P, De Proft F, Langenaeker W (2003) Chem Soc Rev 103:1793–1874
79. Chattaraj PK (2009) Chemical reactivity theory: A density functional view. Taylor & Francis/CRC Press, Florida
80. Damoun S, Van de Woude G, Méndez F, Geerlings P (1997) J Phys Chem A 101:886–893
81. Pinter B, Nagels N, Herrebout WA, De Proft F (2012) Chem Eur J 19:519–530

82. Feng XT, Yu JG, Liu RZ, Lei M, Fang WH, Proft FD, Liu S (2010) J Phys Chem A 114:6342–6349
83. Liu S, Hu H, Pedersen LG (2010) J Phys Chem A 114:5913–5918
84. Huang Y, Liu L, Liu S (2012) Chem Phys Lett 527:73–78
85. Liu S, Parr RG (2007) J Phys Chem A 111:10422–10425
86. Liu S (2007) J Chem Phys 126:244103
87. Thanikaivelan P, Padmanabhan J, Subramanian V, Ramasami T (2002) Theor Chem Accounts 107:326–335
88. Oláh J, Van Alsenoy C, Sannigrahi AB (2002) J Phys Chem A 106:3885–3890
89. Koch U, Popelier PLA (1995) J Phys Chem 99:9747–9754
90. Cubero E, Orozco M, Luque FJ (1999) J Phys Chem A 103:315–321
91. Popelier PLA (2000) Coord Chem Rev 197:169–189
92. Amezaga NJM, Pamies SC, Peruchena NLM, Sosa GL (2010) J Phys Chem A 114:552–562
93. Duarte DR, Vallejos M, Peruchena N (2010) J Mol Model 16:737–748
94. Otero-de-la-Roza A, Luaña VC (2010) J Chem Theory Comput 6:3761–3779
95. Wiberg KB, Bader RFW, Lau CDH (1987) J Am Chem Soc 109:985–1001
96. Timerghazin QK, Peslherbe GH (2007) J Chem Phys 127:064108
97. Duarte DR, Sosa G, Peruchena N (2013) J Mol Model 19:2035–2041
98. Ferreira JAB, Sánchez-Coronilla A, Togashi DM, Ferreira H, Ascenso JR, Costa SMB (2012) J Phys Chem A 116:11938–11945
99. Eskandari K, Zariny H (2010) Chem Phys Lett 492:9–13
100. Wiberg KB (1968) Tetrahedron 24:1083–1096
101. Trindle C (1969) J Am Chem Soc 91:219–220
102. Phukan AK, Guha AK, Silvi B (2010) Dalton Trans 39:4126–4137
103. Chen Z, Wannere CS, Corminboeuf C, Puchta R, Schleyer PVR (2005) Chem Soc Rev 105:3842–3888
104. Wakamiya A, Murakami T, Yamaguchi S (2013) Chem Sci 4:1002–1007
105. Pearson RG (1963) J Am Chem Soc 85:3533–3539
106. Crowe JH, Clegg JS (eds) (1973) Anhydrobiosis. Dowden, Hutchinson and Ross, Stroudsburg
107. Murray JS, Politzer P (2011) Wiley Interdiscip Rev Comput Mol Sci 1:153–163
108. Geng Y, Li HB, Wu SX, Su ZM (2012) J Mater Chem 22:20840–20851
109. Politzer P, Lane P, Concha M, Ma Y, Murray J (2007) J Mol Model 13:305–311
110. Riley KE, Murray JS, Fanfrlík J, Řezáč J, Solá RJ, Concha MC, Ramos FM, Politzer P (2012) J Mol Model. doi:10.1007/s00894-012-1428-x